

## PAPER

Cite this: DOI: 10.1039/c8ta06508j

# Selective extraction of supported Rh nanoparticles under mild, non-acidic conditions with carbon monoxide†

Malek Y. S. Ibrahim and Scott E. Denmark  \*

Owing to their limited supplies, recycling of precious metals, especially rhodium, is vital to sustain the growth of certain nanotechnologies. Here we report a mild, efficient, and selective method for rhodium recovery that relies on the use of carbon monoxide to extract rhodium nanoparticles on various supports in polar solvents. Unlike the traditional recycling technologies, this method operates at low temperature and does not require strong acids. Moreover, the CO-induced leaching is complimentary to leaching by acids in terms of selectivity toward rhodium *versus* other precious metals and results in metal recovery in the form of reduced metallic clusters. The method performs best on freshly reduced surfaces and can be promoted by the addition of tertiary amines. Besides CO gas, formic acid can also be used as a leachant by decomposition to produce CO by Rh catalysis. The concept of CO-induced leaching could be applied to the extraction of rhodium from nuclear waste and extended to modify rhodium nanoparticle size and composition.

Received 6th July 2018  
Accepted 29th August 2018

DOI: 10.1039/c8ta06508j  
[rsc.li/materials-a](http://rsc.li/materials-a)

Owing to their unique catalytic properties, supported Rh nanoparticles (NPs) are widely used as catalysts for carbon monoxide oxidation, selective hydrogenation, formylation, carbon dioxide methanation, and Fisher-Tropsch synthesis.<sup>1–3</sup> Notably, more than 80% of Rh production goes to catalytic converters, which are devices used to treat gaseous emissions from internal combustion engines.<sup>4</sup> In a typical catalytic converter, Rh is often paired with Pd, Pt or both and deposited in the form of nanoparticles on a large surface area metal oxide layer that is contained in a refractory honeycomb structure. The continuing growth of the automotive industry and the stricter regulations on emission levels are expected to increase the need for catalytic converters to the point that the limited Rh supplies will not be able to meet the world demand.<sup>5</sup> Although Rh is generated as a byproduct in nuclear reactors, currently, no method allows for the selective and safe extraction from nuclear waste because of contamination by highly radioactive Ru isotopes.<sup>6</sup>

Several recycling methods have been introduced to extract precious metals from used catalytic converters, however, these methods typically involve melting the catalytic convertor at  $T > 1500$  °C with collector metals such as copper, magnesium, or iron to form alloys with the precious metals that can be separated from the slag containing the ceramic support.<sup>7</sup> Alternatively, a number of hydrometallurgical methods have been proposed based on digesting the spent catalyst in *aqua regia* or other strong oxidizing acids. Elevated temperatures are required because of

strong resistance of Rh to acids.<sup>8–15</sup> In view of the harsh conditions and the corrosive chemicals needed in established methods, the leaching process is often costly, energy demanding, and not environmentally friendly. The severe leaching conditions also result in destruction of the support material and necessitate further purification of the extracted metals.<sup>7</sup>

The need to replace the current recycling methods with more environmentally friendly and sustainable processes is growing in response to the rising public awareness and governmental regulations regarding Earth resources.<sup>16</sup> For this purpose, more elegant methods have been invented for precious metal recovery including dry chlorination of Rh with chlorine gas at 500 °C,<sup>17</sup> digestion in basic cyanide solutions at >100 °C,<sup>18</sup> and more recently, induced surface potential alteration through repetitive cycles of oxidation and reduction with ozone and carbon monoxide for Pt recycling.<sup>19</sup>

In this disclosure we demonstrate the ability of carbon monoxide to induce leaching of Rh NPs as a mild, and non-corrosive way for the selective removal of Rh from supports containing other metals. The leaching efficiency is at highest on freshly reduced Rh NPs and when performed in wet acetonitrile in presence of a tertiary amine. Formic acid can also be used as a leaching agent through the Rh-catalyzed decomposition of  $\text{HCO}_2\text{H}$  to produce CO and  $\text{H}_2\text{O}$ .

## CO-induced leaching of Rh NPs in different solvents

A series of supported Rh NPs were synthesized and submitted to different leaching conditions with CO (see ESI Section 2†).

Roger Adams Laboratory, Department of Chemistry, University of Illinois, Urbana, Illinois, 61801, USA. E-mail: [sdenmark@illinois.edu](mailto:sdenmark@illinois.edu)

† Electronic supplementary information (ESI) available: Characterization data, and additional leaching experiments. See DOI: 10.1039/c8ta06508j

Alumina-supported, metallic Rh(0) NPs in the size range of 1 to 2 nm (RhA-red) was dispersed in different solvents and exposed to CO gas at 20 bar. Less than 10% leaching of Rh was observed in dry, non-polar solvents (hexane, toluene, triethylamine, and methyl *tert*-butyl ether) as indicated by the rhodium content analysis of the alumina support before and after the experiment (Fig. 1). Improved leaching was observed in solvents with dipole moments higher than 1.6 D and reached a maximum in acetonitrile.

Addition of water to the leaching solvents led to a noticeable increase in the leaching efficiency (Fig. 1). The salutary effect of water was more prominent in the less polar solvents that form biphasic mixtures with water. Contrariwise, the acetonitrile-water solution remained homogeneous after saturation with CO and resulted in high leaching (78%) which could be further enhanced by the addition of triethylamine (89% leaching was achieved in acetonitrile/water/triethylamine).

The post-leaching supernatants were pale violet after venting the CO and slowly turned into green upon exposure to air. To examine the effect of water on the nature of the leached Rh species, light absorbance of the post leaching solutions was measured in dry and wet acetonitrile. The similarity in light absorbance in dry and wet acetonitrile suggests that the addition of water does not alter the form at which Rh is extracted (Fig. 4Sa†). To further understand the nature of the Rh extracted species, the alumina support was filtered and the solvent was removed from the filtrate under reduced pressure leaving a Rh-rich brown residue that is soluble in dry acetonitrile. Interestingly, the UV-vis spectrum of the redissolved Rh species

matches with that reported for suspended metallic Rh NP (Fig. 4Sb†).<sup>20</sup>

Infrared (IR) spectra taken on the Rh residue directly after solvent removal showed one major peak in the Rh carbonyl stretching region (2100 to 1600 cm<sup>-1</sup>) at 2024 cm<sup>-1</sup> with two shoulders at 2070 cm<sup>-1</sup> and 1970 cm<sup>-1</sup> and a broad peak at 1843 cm<sup>-1</sup> (Fig. 2a). Exposure of the residue to air led to attenuation of the peak at 2024 cm<sup>-1</sup> relative to the peaks at 2070 cm<sup>-1</sup> and 1970 cm<sup>-1</sup> (Fig. 2b). The IR fingerprint of the residue suggests that the neutral Rh carbonyl clusters Rh<sub>6</sub>(CO)<sub>16</sub> or Rh<sub>4</sub>(CO)<sub>12</sub> are not formed as indicated by the absence of the characteristic strong peaks at 1800 cm<sup>-1</sup> and 2100 cm<sup>-1</sup> of these two species, respectively.<sup>21,22</sup> Additionally, Rh is not extracted in the form of cationic Rh(i) carbonyl species as indicated by the mismatch between the measured IR bands and those reported for [Rh(CO)<sub>2</sub>]<sup>+</sup> surface species or the ligand-stabilized Rh(CO)<sub>2</sub>(MeCN)<sup>+</sup> and Rh(CO)<sub>2</sub>(Et<sub>3</sub>N)<sup>+</sup> species at 2090, 2020 and 2090 to 2002 cm<sup>-1</sup> respectively.<sup>23</sup>

The fingerprint of the post-leaching residue resembles that reported for the double cluster anion [Rh<sub>12</sub>(CO)<sub>(30-34)</sub>]<sup>2-</sup> that contains two [Rh<sub>6</sub>(CO)<sub>16</sub>] units linked by a Rh-Rh bond and two bridging carbonyls (2055, 2010, 1840 cm<sup>-1</sup>).<sup>24</sup> Additionally, the anionic [Rh<sub>6</sub>(CO)<sub>15</sub>]<sup>2-</sup> species (2045, 1980, 1960 cm<sup>-1</sup>) appear to be present in equilibrium with the double cluster [Rh<sub>12</sub>(CO)<sub>30-34</sub>]<sup>2-</sup> as indicated by the shoulder peak at 1970 cm<sup>-1</sup>.<sup>25</sup> Upon air exposure, the residue is transformed to the hydride cluster [Rh<sub>6</sub>(CO)<sub>15</sub>H<sub>(x=1,2)</sub>]<sup>(0=-1,0)</sup> that exhibit peaks at 2060 and 2020 cm<sup>-1</sup>.<sup>25,26</sup> Mass spectroscopy analysis of the post leaching solution shows that Rh is extracted in the form of polynuclear clusters containing 4 to 10 Rh atoms per cluster and around 3 CO/Rh atom in average (Fig. 5S†). Heating the Rh carbonyl clusters under hydrogen atmosphere at 200 °C lead to the formation of metallic powder (93.18 wt% Rh) that does not exhibit any IR bands (Fig. 2c). Additionally, TEM images of the residue collected after solvent removal showed the formation of metallic NPs in the range of 1 to 3 nm (Fig. 2d).

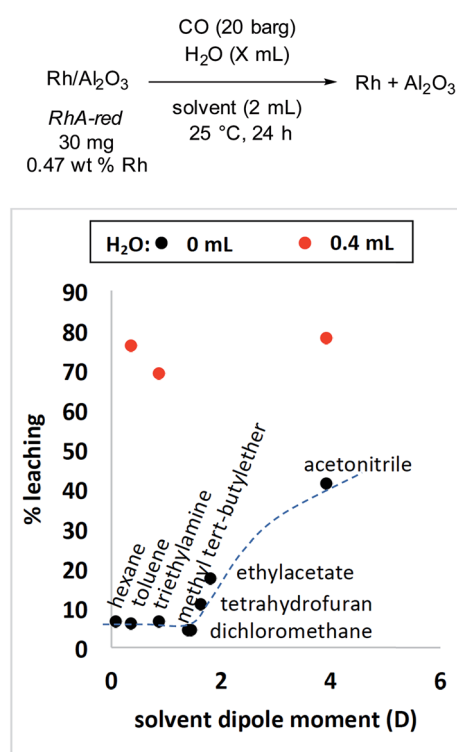


Fig. 1 Leaching of RhA-red sample in different solvents.

## Effect of Rh oxidation and aerobic storage on leaching

NPs of different oxidation states were tested to evaluate the effect the oxidation state on leaching efficiency. A highly oxidized sample (RhA-oxd500) mainly consisting of Rh(i) & (iii) species as indicated by XPS (Fig. 3Sb†) was compared to the reduced sample (RhA-aged1). Despite having similar NP size, no measurable leaching of (RhA-oxd500) was observed below 15 bar CO pressure (Fig. 3). As CO pressure was increased, leaching began gradually with only 7% leaching obtained at 25 bar. Apart from the drop in the leaching efficiency with the oxidized sample, no leaching of either samples occurred in absence of CO, and the introduction of CO at pressures as low as 1 barg was enough to leach 30% of the reduced and stored under air for one month sample (RhA-aged1). This leaching efficiency was increased as leaching was performed under higher CO pressure and reached a maximum of 55% at 15 barg. Beyond this value, no impact on leaching was observed.

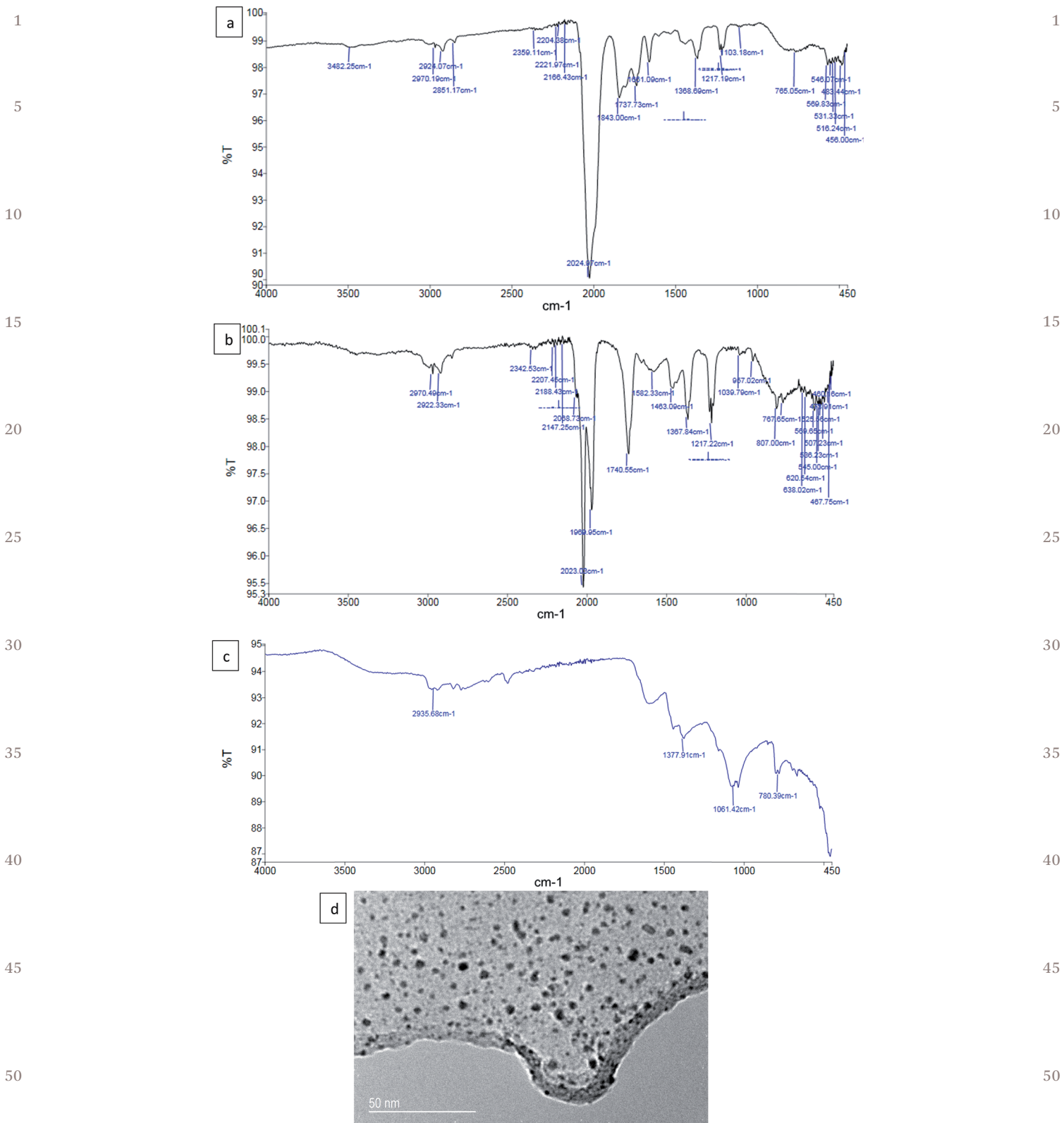


Fig. 2 IR spectra of the post-leaching residue from sample RhA-red (a) after filtration and solvent removal, (b) exposure to air for 10 min, (c) heat treatment at 200 °C under high vacuum, (d) TEM imaging of Rh NPs in post leaching residue.

As indicated by XPS, the storage of the reduced sample RhA-red under ambient air caused the oxidation of Rh(0) to Rh(I) and (III) (Fig. 3SC†) which lead to the observed drop in

the maximum leaching efficiency of sample (RhA-aged1) to 55% compared to the 89% achieved on the same sample before storage.

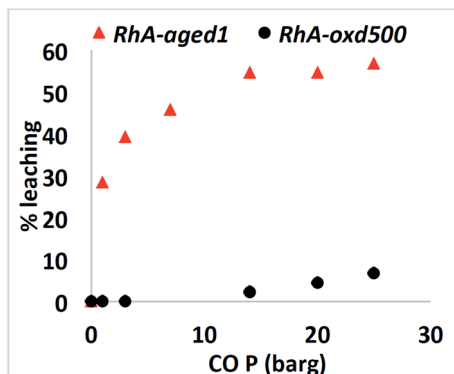
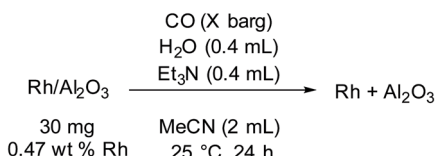


Fig. 3 Effect of CO pressure on leaching of Rh from the pre-reduced and aged (RhA-aged1) sample and the pre-oxidized (RhA-oxd500) in acetonitrile/water/triethylamine solution after 24 h at 25 °C.

Raising the leaching temperature from 25 to 70 to 100 °C increased the leaching efficiency of the highly oxidized (RhA-oxd500) sample from 7 to 11 and 33% respectively (Fig. 4) signifying that leaching of Rh from the highly oxidized sample is inefficient even at elevated temperatures. Notably, the sample (RhA-oxd350) which was oxidized at lower temperature than (RhA-oxd500) showed more efficient leaching (46% at 70 °C, or 4 times higher than (RhA-oxd500)). Additionally, pre-reduction of the highly oxidized sample (RhA-oxd500) directly before

leaching, lead to a 12-fold increase in the leaching efficiency (RhA-oxd/red vs. RhA-oxd500) (Fig. 4).

Furthermore, when submitted to leaching under the same conditions, the sample aged under air for 3 months, RhA-aged3, exhibited significantly less leaching (34% only, Fig. 4) when compared to the sample aged for only 1 month RhA-aged1 (55%, Fig. 3) indicating the continuation in the decay of the leaching efficiency upon samples prolonged storage in air. Nevertheless, the leaching efficiency could be partially recovered by increasing the leaching temperature from 25 to 70 °C (34 to 77%). More importantly, resubmitting sample RhA-aged3 to prereduction directly before leaching (sample RhA-aged/red) lead to an increase in the efficiency from 34 to 74%.

A more densely-loaded commercial sample of Rh NPs supported on alumina (RhA-comm) that contains 4.31 wt% Rh was exposed to the standard leaching conditions at 20 barg CO and 70 °C for 24 hours. This experiment resulted in 50% leaching and thus, leaching was extended for another 48 hour (72 hour total) to achieve 86% leaching. A third leaching stage at room temperature for 24 hour was added to obtain an overall leaching efficiency of 94% as indicated by the final Rh content of 0.24 wt% Rh. The Rh NPs size distribution was measured for the partially extracted sample containing 50% of the original loading and compared to that of the original (RhA-comm) sample. The average particle size was reduced due to leaching from 2.7 to 1.6 nm and the particle size distribution was much narrower (standard deviation drop from 0.75 to 0.4) (Fig. 5).

The distribution of Rh species with different oxidation states was measured on pristine and partially-leached RhA-comm samples. The Rh peaks were deconvoluted using three-component analysis for Rh(0), (i) and (iii) as described in ESI

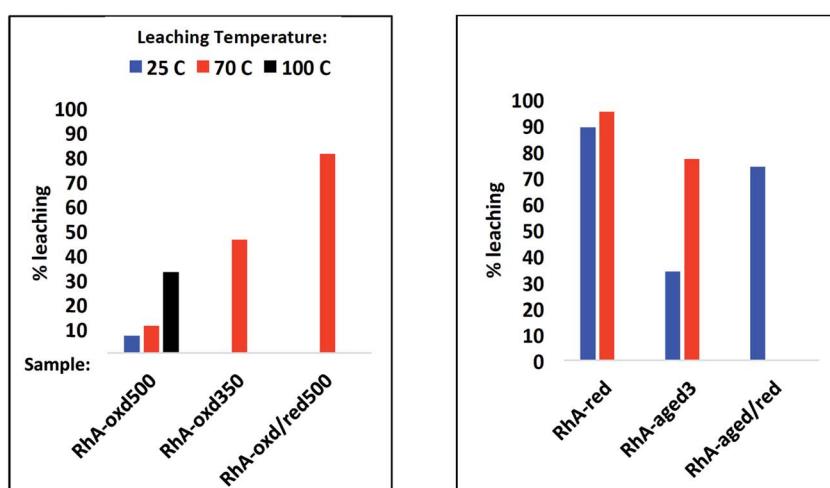
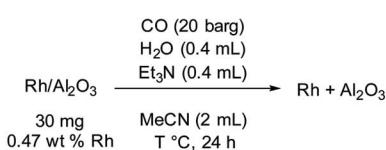


Fig. 4 Effect of temperature on the leaching efficiency of samples pretreated under different conditions. Left: oxidized samples, right: reduced samples.

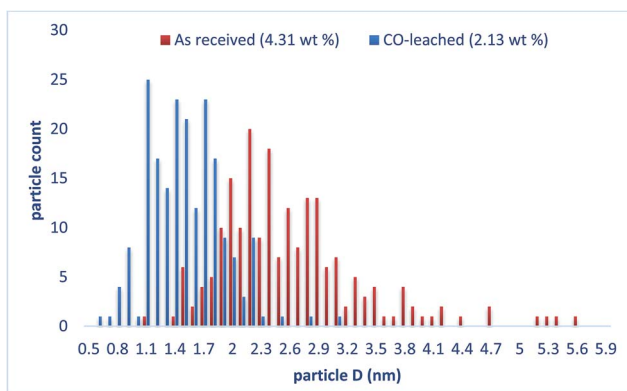


Fig. 5 Effect of CO leaching on nanoparticle size distribution from (RhA-comm) sample.

(Section 3†). Percentages for the different oxidation states of rhodium were estimated from the area of the curves giving the best fitting. Apart from the reduction in the average NPs size and narrowing the size distribution, a decrease in the ratio of the oxidized Rh(I) and (III) species from 21 and 5% to 9 and 3% respectively after leaching was observed (Fig. 6).

## CO-induced leaching of other supported metal nanoparticles

To test the effect of other precious metals on leaching, a mixture of Rh, Pd, Pt, and Ru NPs all supported on alumina was prepared by mixing equal amounts of each individual metal supported NP. The resulting solid mixture was homogenized by grinding and then the sample was reduced under a flow of hydrogen at 500 °C. The leaching experiment of the powder mixture was performed under the standard conditions (20 bar CO, 25 °C, and 24 h) with and without triethylamine. High leaching selectivity for Rh was achieved in absence of triethylamine wherein leaching of Pd and Pt was negligible and leaching of Ru was less than 10% (Fig. 7a). Addition of triethylamine promoted the leaching of Pd to a minor extent but not Rh, Ru, or Pt.

To examine the impact of temperature and pressure on the leaching selectivity for Rh relative to the other metals, the same powder mixture was submitted to leaching at 70 °C under variable CO pressures. No leaching of any of the metals occurred in absence of CO at 70 °C (Fig. 7b). As the CO pressure increased, a rapid increase in the leaching of Rh, Ru and Pd was observed until it leveled off at 7 and 1 barg for Rh and Pd, respectively. Leaching of Ru increased monotonically with CO pressure across the studied range of pressures.

## Rh leaching with CO surrogates

As an alternative to CO gas as a leachant, surrogates that react in presence of Rh to produce CO were also tested. Leaching of the sample stored under ambient air for 1 month (RhA-aged1) was attempted in acetonitrile/water/triethylamine 5 : 1 : 1 solution with the addition of either formic acid, formaldehyde, or carbon dioxide/hydrogen gas mixture in individual experiments. The formic acid and formaldehyde leaching experiments were carried out in a sealed tube at 70 °C for 24 h followed by another 12 h at room temperature before opening the tube. As indicated by the metal content analysis, 80% of the Rh NPs leached with formic acid and less than 10% leached with formaldehyde and carbon dioxide/hydrogen mixture (Table 1, entry 1-3). To examine whether the substantial leaching with formic acid is ascribed to its acidity or its ability to produce CO, the same experiment was run with acetic acid and no leaching was observed. Moreover, suppressing the medium acidity by the addition of super stoichiometric amount of triethylamine did not affect the leaching of Rh with formic acid (Table 1, entry 4 and 5).

## Mechanistic insights on the Rh leaching process

The small size of the CO molecule and its strong affinity to bind to Rh atoms make it an excellent leachant for the metal from porous supports. The best leaching efficiency was observed on a freshly reduced Rh sample in an acetonitrile/triethylamine/

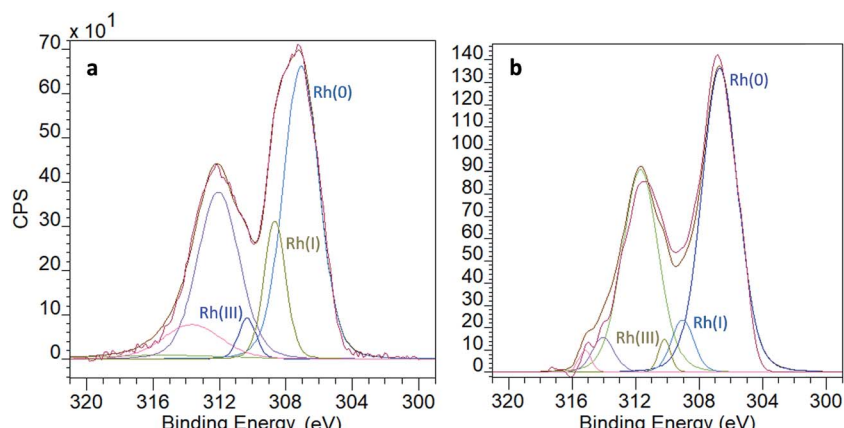
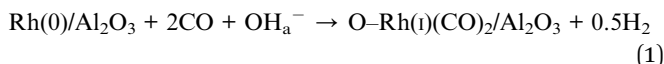


Fig. 6 XPS spectra of commercial Rh NP on alumina RhA-comm (oxidation state distribution from curve fitting) (a) before leaching: 74% Rh(0), 21% Rh(I), 5% Rh(III). (b) After leaching under standard conditions at 70 °C for 72 h followed by another 24 h at 25 °C: 88% Rh(0), 9% Rh(I), 3% Rh(III).

water mixture. Even though both acetonitrile and triethylamine are known to form stable complexes with Rh,<sup>23</sup> no leaching was observed when freshly reduced Rh NP were exposed to a mixture of these two potential leaching agents in absence of CO even at temperature as high as 70 °C. The rate of Rh leaching was found to be dependent on CO pressure as it increased from ambient to 15 barg at 25 °C and from ambient to 7 bar at 70 °C (Fig. 3 and 7). The equilibrium concentration of CO in dry acetonitrile increases linearly with CO pressure in the range of the studied pressures.<sup>27</sup> Thus, the asymptotic behavior of the extent of leaching to further increases in CO pressure beyond these two values cannot be attributed to solvent saturation. Alternatively, the insensitivity of the rate of leaching upon increases in CO pressure could be attributed to the limited rate of the mass transport of CO to the nanoparticle or the diffusion of the formed metal carbonyls through the pores of the support.

Disintegration of Rh NPs by the adsorption of CO gas has been observed by EXAFS and IR measurements in earlier studies.<sup>28–32</sup> The so called “breathing rafts” phenomenon is attributed to the formation of the surface mobile, geminal dicarbonyl Rh(i) species from metallic Rh(0) clusters through the oxidation by the hydroxide ions present on the surface of the support



This reaction is thought to be thermodynamically driven by the large difference in energy between the Rh–CO strong bond (163 kJ mol<sup>−1</sup>) and the weaker Rh–Rh bond (111 kJ mol<sup>−1</sup>).<sup>25</sup> The breathing rafts effect is reversible as indicated by the reformation of metallic Rh(0) clusters upon venting CO and thus the application of this phenomenon was limited to explaining Rh reactivity under vapor phase reactions involving CO.

The mechanism by which the CO-induced leaching of Rh taking place in acetonitrile in this work is less well understood. For example, the unique ability of acetonitrile to promote the leaching cannot solely be attributed to the high solubility of CO in this solvent (0.0053 mol CO per mol acetonitrile at 25 °C and 13 bar).<sup>27</sup> In fact, CO equilibrium concentration in acetonitrile is 5 times less than that of ethyl acetate and 8 to 9 times less than that of alkanes and ethers.<sup>27,33</sup> However, these solvents were inferior to acetonitrile in terms of leaching efficiency. Instead, the high polarity of acetonitrile ( $D = 3.92$ ) and the violet color of the post-leaching solution that turns to green upon air exposure suggest that acetonitrile is essential to stabilize the anionic Rh carbonyl species;  $[\text{Rh}_{12}(\text{CO})_{30}]^{2-}$  (violet), and  $[\text{Rh}_6(\text{CO})_{15}]^{2-}$  (dark green), from the rapid redeposition on the support upon venting CO.<sup>34</sup>

In the breathing rafts phenomenon, the formation of Rh(i)(CO)<sub>2</sub> species was found to be limited by the abundance of surface hydroxide ions.<sup>35–37</sup> In the liquid phase CO-induced leaching, OH<sup>−</sup> ions are continuously replenished by the added water which explains the increase in the leaching efficiency from 41 to 78% when water was added to acetonitrile (Fig. 1). Albeit the ability of hydroxide ions to readily form by the dissociative adsorption on metal oxide surfaces, addition of tertiary amines was found to catalyze the leaching potentially by maximizing the OH<sup>−</sup> concentration. Addition of secondary amine such as piperidine or dibasic amines such as tetramethyl ethylenediamine was found to suppress the leaching (Tables 2S and 6S†) potentially because of the formation of surface stable metal complexes with these additives. On the other hand, inorganic ions commonly present in water including sodium hydroxide, hydrochloric acid, and sodium chloride did not have a significant impact on the leaching efficiency (Table 3S†).

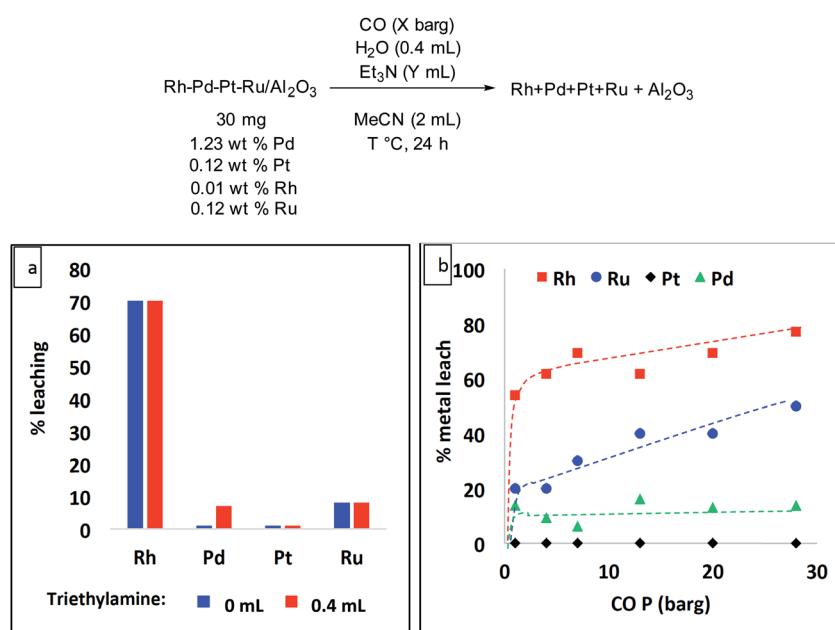
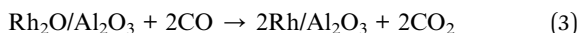
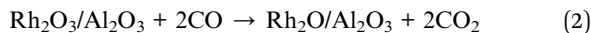


Fig. 7 (a) Selective leaching of Rh in presence of Pd, Pt, and Ru with and without triethylamine at 20 barg CO and 25 °C. (b) Effect of CO pressure on leaching of Rh, Pd, Pt, and Ru from a mixture of the four metals in acetonitrile/water/triethylamine 5 : 1 : 1 v/v/v mixture at 70 °C.

Table 1 Leaching of Rh nanoparticles with CO surrogates

Rh/Al <sub>2</sub> O <sub>3</sub>	additive H <sub>2</sub> O (0.4 mL) Et <sub>3</sub> N (0.4 mL)	Rh + Al <sub>2</sub> O <sub>3</sub>
RhA-aged1 30 mg 0.47 wt% Rh	MeCN (2 mL) 70 °C, 24 h, 25 °C, 12 h	
Additive	% leaching	
HCHO (1 mL)	9	
H <sub>2</sub> (7 bar) + CO <sub>2</sub> (14 bar)	9	
HCOOH (1 mL)	80	
CH <sub>3</sub> COOH (1 mL)	0	
HCOOH (1 mL) + Et <sub>3</sub> N(2 mL)	80	
—	0	

Apart from the mechanism of leaching of Rh(0) metallic NPs with CO, oxidation of the NP lead to a drastic drop in leaching efficiency (Fig. 3). Oxidation by air at temperature as high as 500 °C did not lead to a significant change in the average nanoparticle size (1.8 *vs.* 1.5 nm) and thus, the drop in leaching cannot be attributed to nanoparticles agglomeration. The content of the oxidized Rh(i) and Rh(III) species was 75% in the oxidized sample *versus* 8% only in the freshly reduced sample (Fig. 3S†) which can explain the difference in the resistance towards leaching by CO in these two cases. Although *ca.* 25% of metallic Rh(0) is present in the oxidized sample, the leaching efficiency remained low at 7%. The inability to extract the Rh(0) in presence of the oxidized Rh(i and III) species can be explained by the structure of the oxidized Rh NPs as a Rh(0) core entrapped in a Rh(i) and Rh(III) shell which makes the metallic Rh(0) species inaccessible for CO to bind.<sup>37</sup> The induction of leaching of the oxidized sample RhA-oxd500 at high CO pressure (Fig. 3) and at high leaching temperature (Fig. 4) is probably resulting from the ability of CO to act as a reductant for Rh(i) and Rh(III) through the following reactions:<sup>38</sup>



As the Rh(III) shell is reduced to Rh(i) and Rh(0) the NP becomes prone to leaching by CO. The rate of Rh reduction by CO in acetonitrile/water solution appears to be much slower than that of the leaching of Rh(0) and also to be dependent on the CO pressure along the entire range of the studied pressures (Fig. 3).

## Applications of the leaching process

The commercial sample RhA-comm tested in this study had 10 times more Rh than the synthesized samples and thus it required longer time to achieve appreciable levels of leaching by CO. The longer time needed for leaching can be attributed to the larger average particle size (2.7 nm) and the broader size distribution (0.75 standard deviation). Moreover, spent

heterogeneous Rh catalysts are often transferred and stored under atmospheric air for long time and thus the surface of this kind of nanoparticles is often in the form of Rh(i) and Rh(III). Despite these challenges, higher than 90% leaching was achieved on the commercial sample when tested as received after 4 days of leaching. Upon examining the NP size distribution of a partially leached sample containing half of the original Rh content of the pristine sample, the average particle size was brought down from 2.7 to 1.6 nm and the particle size distribution was much narrower as indicated by their standard deviation (0.4 *versus* 0.75). Besides recycling of metals from spent catalysts, CO-induced leaching can be exploited as a scalable method to narrow the nanoparticle size distribution and enhance their catalytic selectivity.<sup>39</sup>

The ability to extract Rh was extended to nanoparticles supported on titanium oxide (see ESI Section 5.5†) and non-oxide supports as demonstrated in the case of the carbon supported RhC-comm sample (see ESI Section 6.6†). Owing to the mild conditions applied in the CO-induced leaching, destruction of the support is unlikely and thus, recovery of both the metal and the support is possible. The ability to recover the support is economically attractive when highly engineered supports are used such as carbon nanotubes and other nano-shaped structures.<sup>40-42</sup>

Leaching of alumina-supported Pd, and Pt NPs was found to be much less favorable when compared to Rh (Fig. 7). This selectivity can be attributed to the lower stability of the carbonyls of Pt and Pd compared to Rh. Moreover, the calculated difference in the gas phase free energy between the metal cluster and the isolated surface carbonyl monomer is much less for Pd and Pt.<sup>43</sup> Even in the case of the freshly reduced mixture of the un-alloyed nanoparticles, the CO-induced leaching remained highly selective toward Rh indicating the minimal effect of the formed homogeneous Rh carbonyl clusters on catalyzing the leaching of other metals (Fig. 7a). Addition of triethylamine was found to slightly promote the leaching of Pd, nevertheless, the mechanism of the base-mediated leaching of Pd NPs under CO is probably different from that of Rh and for the purpose of this study, it can be concluded that elimination of the tertiary amine from the leaching medium enhances the selectivity of leaching Rh *versus* Pd.

Although Rh extraction from the radioactive nuclear waste is beyond the scope of this study, the ability to selectively extract Rh but not Ru is advantageous in this endeavor.<sup>6</sup> Additionally, the ability to extract Rh in the form of polynuclear clusters could be further exploited to isolate the heavier clusters that are rich in the heavier isotopes by mass centrifugation and bring the radioactivity of the extracted metal to safe levels.

CO-surrogates can be used as an attractive alternative for applications wherein handling high pressure CO gas is troublesome. The success of this process relies on the ability of formic acid to decompose in presence of Rh catalyst to produce CO. In this process, the rate of leaching is expected to be highly dependent on the ability of the Rh catalyst to form CO *in situ*. The unique ability of formic acid to achieve high leaching of Rh from a partially oxidized sample can be attributed to the rapid decomposition of the acid to CO and H<sub>2</sub>O under mild conditions.<sup>44-46</sup>

## Conclusion

An efficient and selective method for extraction of rhodium from different supports using CO in polar solvents had been described. Higher than 90% leaching can be achieved on freshly reduced samples with high selectivity for rhodium in presence of other precious metals. This method produces the metal in the form of highly reduced, polynuclear clusters. Beyond extraction of rhodium from spent catalysts under mild conditions, the reported method has potential applications in extracting rhodium from inaccessible sources and tailoring the size and composition of supported NP to enhance their specific reactivity. In addition to CO, formic acid can also be used as a leachant under mild conditions.

## Authors contributions

M. Y. I. carried out the samples preparation, characterization, and leaching experiments. S. E. D. advised on the experiment and provided input on the data analysis and writing the paper.

## Conflicts of interest

M. Y. Ibrahim and S. E. Denmark are inventors on US provisional patent application no. 62/590,833 filed on November 27<sup>th</sup> 2017.

## Acknowledgements

The research was supported by National Science Foundation (NSF CHE 1649579). Metal content analysis was conducted by the Microanalysis Lab SCS UIUC. TEM and XPS was performed in MRL lab, UIUC.

## References

- Y. Yuan, N. Yan and P. J. Dyson, *ACS Catal.*, 2012, **2**, 1057–1069.
- S. Alayoglu and B. Eichhorn, *J. Am. Chem. Soc.*, 2008, **130**, 17479–17486.
- N. A. Beckers, S. Huynh, X. Zhang, E. J. Luber and J. M. Buriak, *ACS Catal.*, 2012, **2**, 1524–1534.
- P. J. Loferski, *Commodity Report: Platinum-Group Metals (PDF)*, United States Geological Survey, 2014, Retrieved 2017-12-09.
- R. G. Eggert, *Nat. Chem.*, 2011, **3**, 688–691.
- R. P. Bush, *Platinum Met. Rev.*, 1991, **35**, 202–208.
- Z. Peng, Z. Li, X. Lin, H. Tang, L. Ye, Y. Ma, M. Rao, Y. Zhang, G. Li and T. Jiang, *JOM*, 2017, **69**, 1553–1562.
- H. Dong, J. Zhao, J. Chen, Y. Wu and B. Li, *Int. J. Miner. Process.*, 2015, **145**, 108–113.
- T. Suoranta, O. Zugazua, M. Niemelä and P. Perämäki, *Hydrometallurgy*, 2015, **154**, 56–62.
- D. Jimenez de Aberasturi, R. Pinedo, I. Ruiz de Larramendi, J. I. Ruiz de Larramendi and T. Rojo, *Miner. Eng.*, 2011, **24**, 505–513.
- S. Harjanto, Y. Cao, A. Shibayama, I. Naitoh, T. Nanami, K. Kasahara, Y. Okumura, K. Liu and T. Fujita, *Mater. Trans.*, 2006, **47**, 129–135.
- C. A. Nogueira, A. P. Paiva, P. C. Oliveira, M. C. Costa and A. M. R. da Costa, *J. Hazard. Mater.*, 2014, **278**, 82–90.
- C. W. Bradford, S. G. Baldwin, Recovery of Pt/Rh from car exhaust catalysts, *US Pat.*, 3985854, 1976.
- D. Variable, F. Grivon, Process for the recovery of precious metals from used and/or defective catalytic carriers, *US Pat.*, 12847169, 2011.
- V. Shipachev, Wet process and reactor for the recovery of platinum group metals from automobile catalytic converters, *WO 2003010346A2*, 2003.
- S. A. Matlin, G. Mehta, H. Hopf and A. Krief, *Nat. Chem.*, 2015, **7**, 941.
- V. J. F. De, P. M. Chennelles, Process for recovering platinum group metals, *WO 2014091456*, 2014.
- R. S. Bhaduri, H. K. C. Timken, A metallurgical extraction technique to recover platinum group metals from a filter cake, *WO 2016064444*, 2016.
- N. Hodnik, C. Baldizzone, G. Polymeros, S. Geiger, J. P. Grote, S. Cherevko, A. Mingers, A. Zeradjanin and K. J. J. Mayrhofer, *Nat. Commun.*, 2016, **7**, 13164.
- M. Harada and Y. Inada, *Langmuir*, 2009, **25**, 6049–6061.
- P. Chini, *Inorg. Chem.*, 1969, **8**, 1206–1207.
- P. Chini and S. Martinengo, *Inorg. Chim. Acta*, 1969, **3**, 315–318.
- L. D. Rollmann, *Inorg. Chim. Acta*, 1972, **6**, 137–140.
- P. Chini and S. Martinengo, *Inorg. Chim. Acta*, 1969, **3**, 299–302.
- P. Chini, G. Longoni and V. G. Albano, High Nuclearity Metal Carbonyl Clusters, in *Advances in Organometallic Chemistry*, ed. F. G. A. Stone and R. West, Academic Press, 1976, vol. 14, pp. 285–344.
- K. Kiyotomi, F. Kazuo, T. Tetsuya and I. Toshinobu, *Bull. Chem. Soc. Jpn.*, 1991, **64**, 602–612.
- Z. K. Lopez-Castillo, S. N. V. K. Aki, M. A. Stadtherr and J. F. Brennecke, *Ind. Eng. Chem. Res.*, 2006, **45**, 5351–5360.
- P. Basu, D. Panayotov and J. T. Yates, *J. Am. Chem. Soc.*, 1988, **110**, 2074–2081.
- H. F. J. Van't Blik, J. B. A. D. Van Zon, T. Huizinga, J. C. Vis, D. C. Koningsberger and R. Prins, *J. Am. Chem. Soc.*, 1985, **107**, 3139–3147.
- O. S. Alexeev, G. Panjabi, B. L. Phillips and B. C. Gates, *Langmuir*, 2003, **19**, 9494–9503.
- S. Shylesh, D. Hanna, A. Mlinar, X. Q. Kōng, J. A. Reimer and A. T. Bell, *ACS Catal.*, 2013, **3**, 348–357.
- P. Johnston, R. W. Joyner, P. D. A. Pudney, E. S. Shapiro and B. P. Williams, *Faraday Discuss. Chem. Soc.*, 1990, **89**, 91–105.
- J. W. Lorimer, *Solubility Data Series: volume 43, Carbon Monoxide (PDF)*, International Union of Pure and Applied Chemistry, 1990, Retrieved 2018-10-01.
- P. Chini and S. Martinengo, *J. Chem. Soc., Chem. Commun.*, 1969, **19**, 1092–1093.
- P. Basu, D. Panayotov and J. T. Yates, *J. Phys. Chem.*, 1987, **91**, 3133–3136.
- A. Erdöhelyi and F. Solymosi, *J. Catal.*, 1983, **84**, 446–460.

1 37 A. Muñoz, G. Munuera, P. Malet, A. R. González-Elipe and J. P. Espinós, *Surf. Interface Anal.*, 1988, **12**, 247–252.

5 38 C. T. Williams, K. Y. Chen, C. G. Takoudis and M. J. Weaver, *J. Phys. Chem. B*, 1998, **102**, 4785–4794.

10 39 E. C. Tyo and S. Vajda, *Nat. Nanotechnol.*, 2015, **10**, 577.

40 40 J. Ma, R. Hoch, Process for the recovery of catalytic metal and carbon nanotubes, *US Pat.*, 8852547B2, 2014.

41 R. Giordano, P. Serp, P. Kalck, Y. Kihn, J. Schreiber, C. Marhic and J. L. Duvail, *Eur. J. Inorg. Chem.*, 2003, 610–617.

42 M.-L. Kontkanen, M. Tuikka, N. Kinnunen, S. Suvanto and M. Haukka, *Catalysts*, 2013, **3**, 324.

43 B. R. Goldsmith, E. D. Sanderson, R. Ouyang and W. X. Li, *J. Phys. Chem. C*, 2014, **118**, 9588–9597.

44 K. Tedsree, T. Li, S. Jones, C. W. A. Chan, K. M. K. Yu, P. A. J. Bagot, E. A. Marquis, G. D. W. Smith and S. C. E. Tsang, *Nat. Nanotechnol.*, 2011, **6**, 302.

45 G. A. Papapolymerou and L. D. Schmidt, *Langmuir*, 1987, **3**, 1098–1102.

46 C. Houtman and M. A. Barteau, *Surf. Sci.*, 1991, **248**, 57–76.

15

1

20

5

25

25

30

30

35

35

40

40

45

45

50

50

55

55